Nanoscale Assemblies

DOI: 10.1002/anie.200903910

A Spherical 24 Butyrate Aggregate with a Hydrophobic Cavity in a Capsule with Flexible Pores: Confinement Effects and Uptake–Release Equilibria at Elevated Temperatures**

Christian Schäffer, Hartmut Bögge, Alice Merca, Ira A. Weinstock, Dieter Rehder, Erhard T. K. Haupt, and Achim Müller**

Dedicated to Professor Martin Jansen on the occasion of his 65th birthday

Compounds like zeolites exhibiting nanoscale holes and channels can serve as filters and traps or hosts for molecular guests. They play an important role in many areas of chemistry and materials science as they can be used for different tasks, for example, for separation and storage purposes.[1,2] Our related interest concerns molecular (i.e., discrete) porous metal oxide based capsule analogues, which specifically allow encapsulation of a large number of different guests; for general remarks regarding inorganic host–guest chemistry, see Ref. [3]. It was our aim to integrate within a capsule's cavity an unprecedented structurally well-defined, mostly hydrophobic aggregate. This goal was achieved with a robust, spherical, porous capsule of the type $[\{\text{pentagon}\}_{12}\{\text{linker}\}_{30}] \equiv [\{(Mo)Mo_5O_{21}(H_2O)_6\}_{12}\{Mo_2O_4(\text{ligand})\}_{30}]^{n-}$ [4–7] allowing, generally speaking, a wide range of applications.[4e,f,8] The capsules' interiors can be modified by introducing a variety of species coordinating weakly to the 30 dinuclear $\{Mo_2\}$ linkers. This approach has now allowed, as intended, the encapsulation of the quasi-spherical, partly compact 24 butyrate aggregate, whose constituents show under the confined conditions interesting interactions (an attractive, up-to-date research field) detectable by ROESY NMR spectroscopy in agreement with the related distances. Remarkably, the present scenario automatically generates an unprecedented hydrophobic cavity and shell at the center of the capsule that is spanned by 72 H atoms originating from 24 butyrate CH_3 groups. Furthermore, the resulting capsule skeleton is stable even at rather high temperatures, which allows the observation of a strong uptake–release exchange of the butyrates with the future option to introduce into the capsule system different species that can react with one another under confined conditions. The pictorial title "flexible" refers to one of the important properties of the capsules, that is, the option of reversible pore widening, which will be discussed in comparison with formally related scenarios of spherical viruses.

Compound **1** containing the capsule **1a** loaded with the 24 butyrate aggregate (Figure 1) is obtained by the reaction of an aqueous solution of heptamolybdate with hydrazinium sulfate (as reducing agent) and butyric acid and a subsequent recrystallization process. (The product's recrystallization was primarily performed to obtain higher-quality crystals.) This synthetic procedure is similar to that which led to the first published related capsule-type compound with 30 acetate ligands obtained in a facile high-yield synthesis,[7] while the

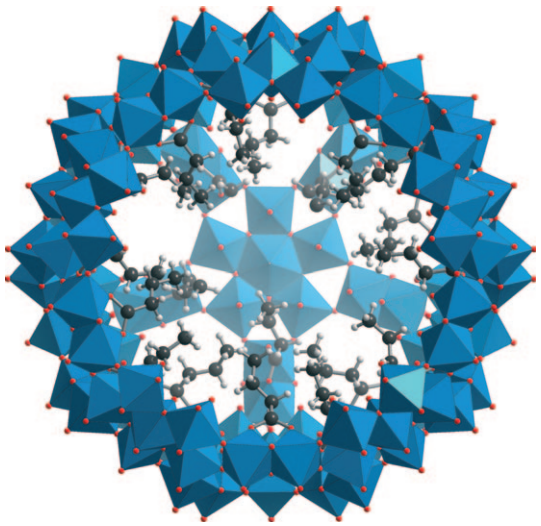

Figure 1. Structure of the capsule **1a** showing details of the butyrate ligands coordinated to the $\{Mo_2\}$-type linkers (see Figure 2 highlighting the packing of the encapsulates). For clarity, one of the 12 pentagonal $\{(Mo)Mo_5O_{21}(H_2O)_6\}^{6-}$ units and five of the $\{Mo_2O_4(\text{butyrate})\}^{+}$ linkers (polyhedral representation in blue) are omitted; O red, C black, H gray. The H atoms were generated here and in the subsequent figures.

[*] Prof. Dr. D. Rehder, Dr. E. T. K. Haupt
Department Chemie, Institut für
Anorganische und Angewandte Chemie, Universität Hamburg
20146 Hamburg (Germany)
E-mail: erhard.haupt@uni-hamburg.de
C. Schäffer, Dr. H. Bögge, Dr. A. Merca, Prof. Dr. A. Müller
Fakultät für Chemie, Universität Bielefeld
Postfach 100131, 33501 Bielefeld (Germany)
Fax: (+49) 521-106-6003
E-mail: a.mueller@uni-bielefeld.de
Homepage: http://www.uni-bielefeld.de/chemie/ac1/
Prof. Dr. I. A. Weinstock
Department of Chemistry, Ben Gurion University of the Negev
Beer Sheva, 84105 (Israel)

[**] We thank Dr. René Thouvenot and Prof. Pierre Gouzerh (Paris) for discussions. A.M. thanks the Deutsche Forschungsgemeinschaft (E.T.K.H. in context with HA 2822/1-1) and the Fonds der Chemischen Industrie for continuous financial support.

Supporting information for this article is available on the WWW under http://dx.doi.org/10.1002/anie.200903910.

materials properties of the compound and its derivatives were studied by several groups in the meantime (see especially reviews in Refs. [4e,f,5d,e]). Capsule **1a** contains fewer internal ligands (i.e., 24) than the acetate-type capsule, whereas each missing bidentate butyrate ligand is replaced by two H_2O ligands coordinated to a $\{Mo_2\}$ linker (see formula and Figure 1); the reason for the presence of a smaller number of ligands is that the comparably long butyrate chains lead to space limitations in the central part of the capsule.

$$(NH_4)_{16}[(NH_4+H_2O)_{20}\subset\{\{(Mo^{VI})Mo^{VI}{}_5O_{21}(H_2O)_6\}_{12}\{Mo^{V}{}_2O_4(CH_3CH_2CH_2COO)\}_{24}\{Mo^{V}{}_2O_4(H_2O)_2\}_6\}]\cdot$$
$$\text{ca.}\{230\,H_2O+CH_3CH_2CH_2COONH_4\}\equiv$$
$$(NH_4)_{16}\cdot\mathbf{1a}\cdot\text{lattice ingredients}\equiv\mathbf{1}$$

Compound **1** crystallizes in the space group $R\bar{3}$ and was characterized by elemental analyses (including the determination of the crystal water release), redox titration (to determine the number of Mo^V centers), spectroscopic methods (IR, Raman, and especially NMR spectroscopy), and single crystal X-ray structure analysis,[9] including bond valence sum (BVS) calculations.[10] The capsule **1a** has the spherical skeleton (Figure 1)[4–7] mentioned above but exhibits an unprecedented internal structural feature in the form of the partly compact spherical 24 butyrate aggregate (Figure 2), which shows interesting interactions (for details, see Figure 3, top, and text below). The reason why only 24 butyrates are placed inside the capsule is explained in Figure 3, bottom right, whereas the consequential scenario with the densely packed 24 CH_3 groups leads to a shell spanned by 72 H atoms (Figure 3, bottom left). An indication of the hydrophobicity of the central cavity area is that no water molecules could be detected there (see also below), in contrast to all earlier reported capsule types, including that containing acetate ligands.[7c] On the other hand, a water molecule is found along with a NH_4^+ ion[11a] in each of the 20 pores of the capsule. Importantly, the NH_4^+ ions are attracted by the high negative capsule charge (Figure SI-1 in the Supporting Information).

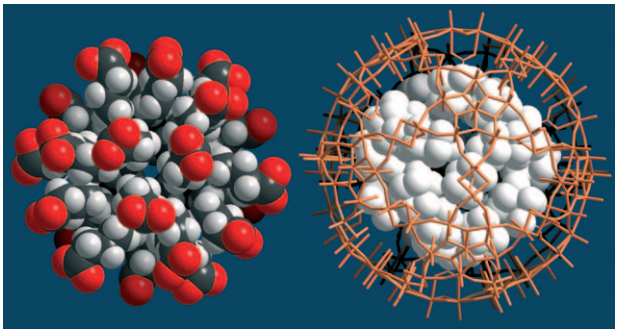

Figure 2. Left: Space-filling representation of the organic 24 butyrate core in **1a** demonstrating the loading of the capsule cavity, while each butyrate interacts only weakly with one of the 24 $\{Mo_2\}$ linkers. Right: All 24×7 H atoms of the butyrates in the capsule cavity (skeleton in wire-frame representation); color code as in Figure 1.

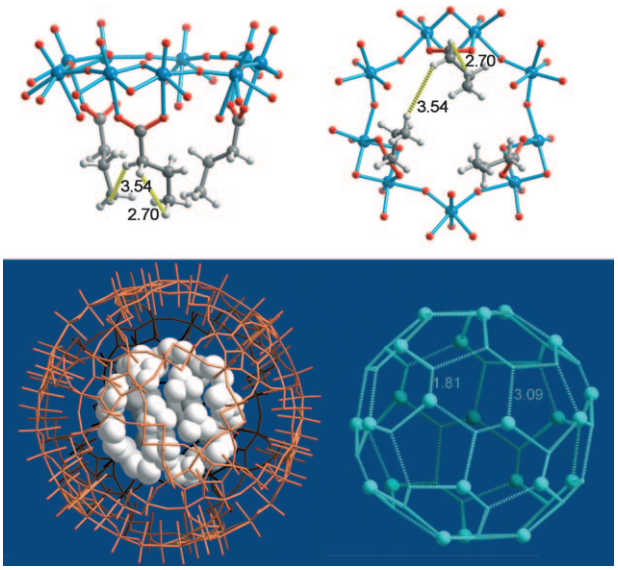

Figure 3. Top: One $\{Mo_9O_9\}$ pore in two views with the corresponding short channel formed by three butyrate ligands showing characteristic distances between the H atoms (in Å) arising from the confinement conditions (see text concerning the related NMR spectroscopy results). Bottom left: Internal shell in the central hydrophobic cavity (diameter ca. 6.2 Å) spanned by the 72 H atoms of the densely packed 24 CH_3 groups in space-filling representation (shortest C···C separation ca. 4.10 Å and shortest H···H distance ca. 2.40 Å; capsule skeleton in wireframe representation). Bottom right: Explains the presence of two sets of only 24 disordered butyrates (instead of 30 related to the 30 $\{Mo_2\}$-linker coordination sites), that is, two per linker in the ratio 1:1 (illustration of a complicated scenario). The shown formal fullerene-type arrangement (12 regular pentagons, distorted hexagons) is constructed by 60 C atoms according to 2×30 positions found under-occupied (with ca. 40% occupation corresponding to 24 butyrates). The shown distance of 1.81 Å formally corresponds to methyl groups of two disordered butyrates belonging to the same $\{Mo_2\}$ linker, while the short 3.09 Å distance indicates that only two methyl C atoms (large spheres) can be positioned at a given pentagon. Consequently, there is only space for 24 (i.e. 12×2) butyrate ligands in the cavity; Mo blue, O red, C positions cyan, H gray; cyan lines indicate formally the above-mentioned interatomic correlation.

The spherical 24 butyrate aggregate filling the capsule cavity (Figure 2, left) warrants—with respect to the confinement conditions—detailed study by ^1H and ^{13}C NMR spectroscopy. Whereas the freshly prepared aqueous solution of **1** obtained after recrystallization contains almost no "free butyrates"[11b] in the crystal lattice (see the Experimental Section and the formula above), the originally precipitated compound (**1′**) contains five of these. The result is obtained by NMR spectroscopy (see Figure 4 and the Supporting Information), that is, by comparison of the related peak intensities relative to those of the 24 internal butyrates of **1** as well as from several elemental analyses. This situation means that recrystallization leads to the removal of most of the external butyrates. All 2D NMR spectroscopy measurements were performed on solutions of **1′** in D_2O in the presence of appropriate amounts of free butyrates, as the corresponding peaks facilitate comparative interpretations and the study of the corresponding exchange equilibria. (The same results were obtained by adding an appropriate amount of butyrate

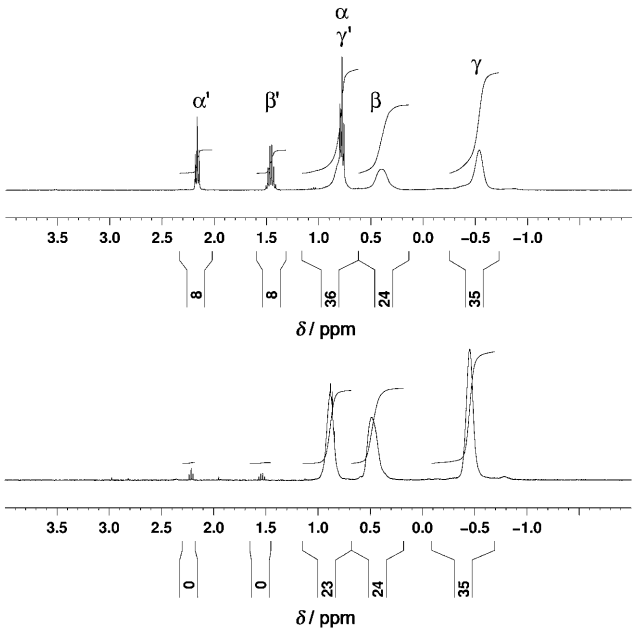

Figure 4. Low-frequency range of the room-temperature ^{1}H NMR spectra in D_2O of **1′** (top trace) and of **1** (with free butyrates reduced to a residual amount after recrystallization of **1**; bottom trace). See Figure SI-2 in the Supporting Information for temperature dependence. Assignment of the three butyrate signals from right to left: CH_3 (γ), CH_3CH_2 (β), $CH_2CO_2^-$ (α). Primed signals correspond to external butyrates (note the overlap of the peaks for C_α and $C_{\gamma'}$); for concentrations used for the measurements of all NMR spectra, see the Supporting Information.

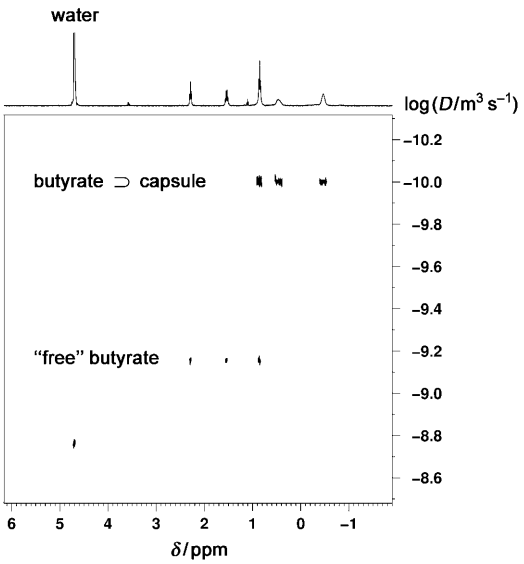

Figure 5. ^{1}H DOSY NMR spectrum of **1′** in D_2O at room temperature. The scale on the right-hand side indicates the diffusion coefficients on a logarithmic scale.

to a solution of **1**.) Important in this context: From analysis of the ^{1}H and ^{13}C NMR spectra (Figure 4 and the Supporting Information), it turns out that the capsules of **1** and **1′** are identical with respect to their interiors, that is, regarding the presence of the encapsulated 24 butyrate aggregate. The fact that the signals for confined butyrates are broadened compared to those of the "free" ones (Figure 4) should be partly due to the quasi-polycrystalline nature of the encapsulated aggregate showing the interactions mentioned below; in any case, peak broadening is generally observed for encapsulated species, such as acetates. The lower-frequency chemical shifts of the ^{1}H signals of the encapsulated butyrates relative to those of the external ones correspond to earlier observations with other capsule–ligand scenarios.[11c]

The presence of internal and free butyrates in **1′** is nicely confirmed by ^{1}H DOSY NMR spectroscopy (Figure 5). The signals attributed to the former—that is, moving with the capsule—exhibit, as expected, the smaller diffusion coefficient; as time-consuming calibration was not performed, we only refer to the values seen in Figure 5 from which an approximate calculation of the hydrodynamic capsule radius is obtained, which is comparable to that found by X-ray crystallography. The DOSY spectra shown in Figure SI-3 in the Supporting Information support that **1a** is even stable at fairly high temperatures (the change of the diffusion coefficients with temperature can also be seen from Figure SI-3 in the Supporting Information). The same follows from the standard variable-temperature (VT) measurements (see Figure SI-2 in the Supporting Information), which do not show any significant variations of the signal shapes and patterns upon heating up to 373 K. (Measurements up to this high temperature were performed in an—unsuccessful—attempt to determine the informative coalescence temperature.)

The interesting interactions of the constituents of the 24 butyrate aggregate based on the confined conditions could be—besides from the ^{13}C NMR spectra of solutions of **1** showing characteristic splittings (see the Supporting Information with Figure SI-4)—especially demonstrated by a room-temperature ROESY spectrum (Figure 6b). While for both types of butyrates the expected peak correlation series $CH_3(\gamma)\rightleftarrows CH_3CH_2(\beta)\rightleftarrows CH_2CO_2^-(\alpha)$ is observed (Figure 6), we obtain for the encapsulated species additional remarkable correlations between CH_3 (H at C_γ) and $CH_2CO_2^-$ (H at C_α) (Figure 6b). This finding might, in principle, be traced back to increased spin diffusion, but the more acceptable interpretation is that these peaks are due to the related contacts between the butyrates, while the ROESY peaks are due to contacts of adjacent chains as well as of the same butyrate chain, with an unknown contribution ratio; from the distances shown in Figure 3 (top), this result was to be expected. Upon slightly increasing the temperature (325 K), the ROEs for the free butyrates vanish owing to an increase in their mobility, but those for the encapsulated ones can, as expected, still be observed (Figure 7a).

One interesting discovery is the uptake–release process of the butyrates observed after further increasing the temperature to 373 K (this behavior was not observed, for instance, at 353 K). The ROESY spectrum at this temperature (Figure 7b) is significantly different from that at lower temperatures—especially from that at room temperature (Figure 6b)—and turns out to be a clear EXSY-type spectrum. Whereas the interchain correlation peaks are of negligible intensity, the spectrum is now dominated by a set

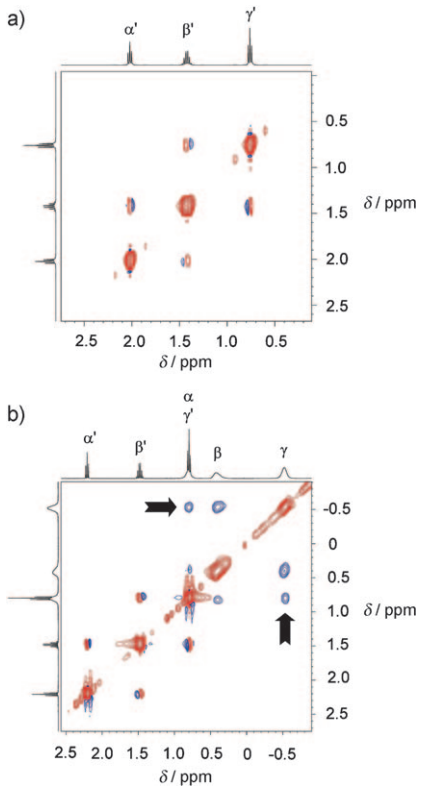

Figure 6. Comparison of the room-temperature (293 K) ROESY spectrum of an aqueous solution of a) sodium butyrate and b) **1′** (right) containing signals of the butyrates in the capsule interior (broad) and the external ones. The nondiagonal peaks in (b) for the two types of correlations (intra- and interchain) between CH_3 and $CH_2CO_2^-$ of confined butyrates are indicated by arrows (negative ROE cross-peaks in blue relative to the positive diagonal peaks in red; for details see reference [17]).

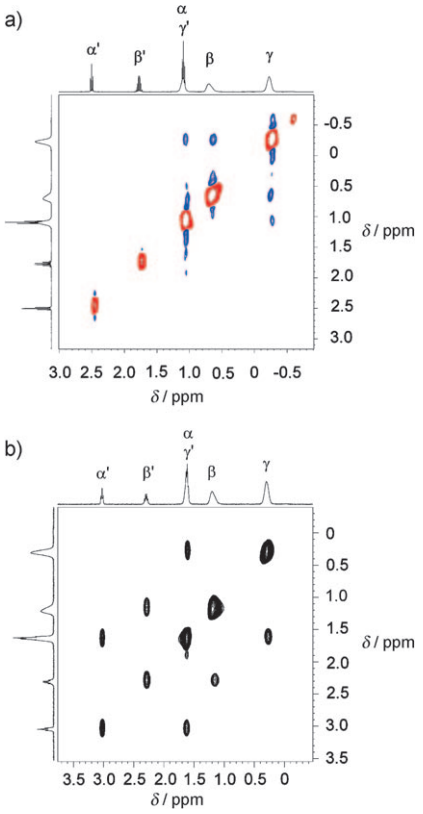

Figure 7. ROESY spectra of **1′** in D_2O at a) 325 and b) ca. 373 K. In both cases, the left group of signals (between $\delta = 2.5$ and 1 ppm) corresponds to free butyrates, the right group of signals (between $\delta = 1$ and -0.5 ppm) to encapsulated butyrates. Chemical shift differences with respect to Figure 6 are due to their temperature dependence. In the left part of (a), the ROESY peaks of the external butyrates are missing owing to an increased mobility after heating to 325 K. Though the ROESY peaks for the encapsulated butyrates are still visible at 325 K owing to their still hindered mobility inside the capsule, they are no longer visible after further temperature increase to ca. 373 K (b), while the spectrum changes from a ROESY to an EXSY spectrum (this temperature corresponds to the highest one used for the VT and DOSY experiments; see above for relevant arguments in the text). Thus, a fascinating chemical exchange of the internal with the external butyrates on the timescale of the experiment is observed (see text). Blue signals negative, red signals positive; color coding has been neglected in the bottom figure because all signals have the same sign.

of three groups of exchange signals of the type α⇄α′, β⇄β′, and γ⇄γ′, which demonstrates that at approximately 373 K (in contrast to lower temperatures), a substantial amount of butyrate exchange (within an equilibrium) between the interior and the exterior takes place. (Lowering the temperature leads to the initial state, as indicated by the ROESY spectrum.) The process is based on very weakly coordinated butyrate ligands but also on at least a small degree of pore widening, as the carboxylate groups of the butyrates are considered to be larger than the pore openings (for details, see Ref. [12a]). After related earlier qualitative observations of capsule pore widening,[12b] this phenomenon was especially shown in a recent kinetic study.[12c] The flexibility of the capsules in connection with the option of pore widening is due to the presence of 120 comparably weak metal–ligand bonds between the Mo atoms of the linkers and the O atoms belonging to the pentagonal $\{(Mo)Mo_5O_{21}(H_2O)_6\}^{6-}$ units; a similar (more easily understandable) situation exists in the case of the analogous capsule Keplerate $[Fe_{30}\{(Mo)Mo_5\}_{12}]$, which exhibits 120 weak Fe···O type metal–ligand interactions, with the 12 pentagonal units considered as ligands.[13] (The strength of the metal–ligand bond decreases with decreasing positive linker charge, which is much smaller in the case of **1a**, namely +1, than in the last-mentioned Keplerate.) Notably, exchange is favored by the presence of protonated species in solution,[12b] which is the case in the present experiments (solution pH ≈ 4.0).[11b] Interestingly, the situation of pore widening can formally be compared with scenarios of spherical viruses, which are formed by assembly processes with the fundamental participation of (as here) 12 pentagonal subunits.[7c] The viruses can undergo reversible structural changes that open or close pores, thus allowing access to their interior,[14] while the mentioned term swelling (or "swollen") can also be formally applied here. Whereas in the latter case hydrogen-bond weakening is involved, in the present case weakening refers to the metal–ligand bonds (for the analogy of the two bond types in supramolecular chemistry, see Ref. [15]).

To summarize:

1) The 24 butyrate unit—rather stable at room temperature—is an unprecedented large partly compact aggregate and can be investigated under confined conditions with the option of extension to other comparably large organic species.
2) In the central part of the 24 butyrate aggregate there is a spherical hydrophobic cavity created by the presence of a shell spanned by the 72 H atoms of the 24 CH_3 groups (for the interesting aspects of hydrophobic cavities, even with water encapsulation, in protein research, see Ref. [18]).
3) The capsule skeleton **1a** is stable up to approximately 370 K in aqueous solutions—probably in part owing to its loading with the hydrophobic material. At that temperature, butyrate uptake–release exchange is observed based on increasing pore flexibility and butyrate ligand mobility.
4) The confinement condition for the 24 butyrate aggregate gives rise to ROE-detectable contacts. The investigation of organic moieties encapsulated in various types of organic cages is a matter of current interest,[16] sometimes found in the literature under the headlines "nanolabs", "nanotubes", and "molecular flasks".

A consequence of the present discovery is that it allows for the study of interactions as well as reactions between different species in the capsule at higher temperatures.

Experimental Section

Preparation of **1**: Butyric acid (15 mL, 14.4 g, 163.4 mmol) and aqueous ammonia solution (12 mL, 25 %) were added to a solution of $(NH_4)_6Mo_7O_{24}\cdot 4H_2O$ (5.6 g, 4.5 mmol) in water (250 mL). After addition of $(N_2H_6)SO_4$ (0.8 g, 6.1 mmol), the solution was stirred for 15 min (color change from colorless to blue-green), and butyric acid (85 mL, 81.6 g, 926.1 mmol) was subsequently added. After the pH value of the solution was adjusted to 3.9 by dropwise addition of hydrochloric acid (30 mL, 2 M), the reaction mixture was stirred for 2 h and then stored in an open 600 mL beaker at room temperature (fumehood; slow color change to dark brown). After five days the precipitated dark brown crystals (**1′**) were filtered off, washed with 80 % ethanol, and dried in air (yield: 5.2 g; 79 % based on Mo). Suitable crystals for X-ray diffraction were obtained by recrystallization: The precipitated compound (1 g) was dissolved in water (60 mL) with the addition of NH_4Cl (1 g). After storing the solution for 3–4 days in an open beaker at room temperature, the precipitated crystals of **1** were filtered off. Elemental analysis for **1** (%, with 180 crystal water) calcd: C 4.52, N 1.95, H 3.38; found: C 4.9, N 2.4, H 2.9 (redox titration 60 ± 2 Mo^V). The formula of **1** corresponds (crystallographically) to full H_2O occupation of all related crystallographic sites, but the calculated values are based on 180 H_2O (actual value for the performed analyses), because the compound slowly loses part of the crystal water when removed from the mother liquor. Characteristic major IR bands (KBr pellet): $\tilde{\nu} = 1622$ (m) [$\nu(H_2O)$], 1535 (m) [$\nu_{as}(COO)$], 1402 (s) [$\nu_{as}(NH_4^+)$], 969 (s) [$\nu(Mo{=}O)$], 853 (m-s), 792 (s), 723 (s), 628 (s), 567 cm^{-1} (s). Characteristic Raman bands (solid state/KBr dilution; $\lambda_e = 1064$ nm): $\tilde{\nu} = 954$ (w), 947 (w) [$\nu(Mo{=}O_{term})$], 877 (vs) [$\nu(\{Mo_2\}O_{bri})$ breathing], 373 (m), 303 cm^{-1} (w).

For the special conditions of the NMR spectroscopy measurements, see the Supporting Information (no. 7).

Received: July 16, 2009
Published online: September 22, 2009

Keywords: confinement effect · NMR spectroscopy · hydrophobic effect · polyoxometalates · porous capsules

[1] *Handbook of Porous Solids, Five Vols.* (Eds.: F. Schüth, K. S. W. Sing, J. Weitkamp), Wiley-VCH, Weinheim, **2002**.
[2] *Comprehensive Supramolecular Chemistry*, *Vol. 7* (Eds.: J. L. Atwood, J. E. D. Davies, D. D. MacNicol, F. Vögtle), Pergamon, Oxford, **1996**.
[3] a) A. Müller, H. Reuter, S. Dillinger, *Angew. Chem.* **1995**, *107*, 2505 – 2539; *Angew. Chem. Int. Ed. Engl.* **1995**, *34*, 2328 – 2361; b) P. N. W. Baxter in *Comprehensive Supramolecular Chemistry*, *Vol. 9* (Eds.: J. L. Atwood, J. E. D. Davies, D. D. MacNicol, F. Vögtle), Pergamon, Oxford, **1996**, pp. 165 – 211; see also c) D. H. Busch, A. L. Vance, A. G. Kolchinski in *Comprehensive Supramolecular Chemistry*, *Vol. 9* (Eds.: J. L. Atwood, J. E. D. Davies, D. D. MacNicol, F. Vögtle), Pergamon, Oxford, **1996**, pp. 1 – 42.
[4] a) L. Cronin in *Comprehensive Coordination Chemistry II*, *Vol. 7* (Eds.: J. A. McCleverty, T. J. Meyer), Elsevier, Amsterdam, **2004**, pp. 1 – 56; b) D.-L. Long, L. Cronin, *Chem. Eur. J.* **2006**, *12*, 3698 – 3706; c) L. Cronin, *Angew. Chem.* **2006**, *118*, 3656 – 3658; *Angew. Chem. Int. Ed.* **2006**, *45*, 3576 – 3578; d) D.-L. Long, L. Cronin, *Chem. Soc. Rev.* **2007**, *36*, 105 – 121; e) A. Proust, R. Thouvenot, P. Gouzerh, *Chem. Commun.* **2008**, 1837 – 1852; f) P. Gouzerh, M. Che, *Actual. Chim.* **2006**, *298*, 9 – 22; g) M. T. Pope in *Comprehensive Coordination Chemistry II*, *Vol. 4* (Eds.: J. A. McCleverty, T. J. Meyer), Elsevier, Amsterdam, **2004**, pp. 635 – 678; h) M. T. Pope in *Encyclopedia of Inorganic Chemistry*, *Vol. VII*, 2nd ed. (Ed.: R. B. King), Wiley, Chichester, **2005**, pp. 4575 – 4586.
[5] a) A. Müller, P. Kögerler, C. Kuhlmann, *Chem. Commun.* **1999**, 1347 – 1358; b) A. Müller, S. Roy, *Coord. Chem. Rev.* **2003**, *245*, 153 – 166; c) A. Müller, S. Roy in *The Chemistry of Nanomaterials: Synthesis Properties and Applications* (Eds.: C. N. R. Rao, A. Müller, A. K. Cheetham), Wiley-VCH, Weinheim, **2004**, pp. 452 – 475; d) A. Müller, S. Roy, *Eur. J. Inorg. Chem.* **2005**, 3561 – 3570 (micro review); e) A. Müller, S. Roy, *J. Mater. Chem.* **2005**, *15*, 4673 – 4677.
[6] M. Gross, *Chem. Br.* **2003**, *39*, 18 and *Chemistry World* **2004**, *1*, Nov. Issue, 18.
[7] a) L. Cronin, E. Diemann, A. Müller in *Inorganic Experiments* (Ed.: J. D. Woollins), Wiley-VCH, Weinheim, **2003**, pp. 340 – 346; b) A. Müller, S. K. Das, E. Krickemeyer, C. Kuhlmann, *Inorg. Synth.* **2004**, *34*, 191 – 200 (Ed.: J. R. Shapley); c) A. Müller, E. Krickemeyer, H. Bögge, M. Schmidtmann, F. Peters, *Angew. Chem.* **1998**, *110*, 3567 – 3571; *Angew. Chem. Int. Ed.* **1998**, *37*, 3359 – 3363.
[8] a) E. T. K. Haupt, C. Wontorra, D. Rehder, A. Müller, *Chem. Commun.* **2005**, 3912 – 3914; b) A. Müller, D. Rehder, E. T. K. Haupt, A. Merca, H. Bögge, M. Schmidtmann, G. Heinze-Brückner, *Angew. Chem.* **2004**, *116*, 4566 – 4570; *Angew. Chem. Int. Ed.* **2004**, *43*, 4466 – 4470; erratum: A. Müller, D. Rehder, E. T. K. Haupt, A. Merca, H. Bögge, M. Schmidtmann, G. Heinze-Brückner, *Angew. Chem.* **2004**, *116*, 5225; *Angew. Chem. Int. Ed.* **2004**, *43*, 5115; c) D. Rehder, E. T. K. Haupt, H. Bögge, A. Müller, *Chem. Asian J.* **2006**, *1–2*, 76 – 81; d) A. Merca, E. T. K. Haupt, T. Mitra, H. Bögge, D. Rehder, A. Müller, *Chem. Eur. J.* **2007**, *13*, 7650 – 7658; e) A. M. Todea, A. Merca, H. Bögge, T. Glaser, L. Engelhardt, R. Prozorov, M. Luban, A. Müller, *Chem. Commun.* **2009**, 3351 – 3353.
[9] Crystal data for **1:** $Mo_{132}C_{100}H_{991}N_{37}O_{756}$, $M = 27\,478.38$ g mol^{-1}, rhombohedral, space group $R\bar{3}$, $a = 32.588(1)$, $c = 73.169(4)$ Å, $V = 67\,294(5)$ Å^3, $Z = 3$, $\rho = 2.034$ g cm^{-3}, $\mu = 1.886$ mm^{-1}, $F(000) = 40\,326$, crystal size $= 0.50 \times 0.40 \times 0.40$ mm^3. Crystals of **1** were removed from the mother liquor and immediately cooled to 188(2) K on a Bruker AXS SMART diffractometer (three-circle goniometer with 1 K CCD detector, Mo_α radiation,

graphite monochromator; hemisphere data collection in ω at 0.3° scan width in three runs with 606, 435, and 230 frames (ϕ = 0, 88, and 180°) at a detector distance of 5 cm). A total of 112333 reflections ($1.50 < \theta < 26.99°$) were collected, of which 31470 reflections were unique (R(int) = 0.0664). An empirical absorption correction using equivalent reflections was performed with the program SADABS 2.10. The structure was solved with the program SHELXS-97 and refined using SHELXL-97 to R = 0.0591 for 23910 reflections with $I > 2\sigma(I)$, R = 0.0869 for all reflections; max/min residual electron density 2.417 and −0.925 e Å^{-3}. (SHELXS/L, SADABS from G. M. Sheldrick, University of Göttingen, **1997/2003**; structure graphics with DIAMOND 3.0, http://www.crystalimpact.com/and with POV-Ray 3.6, http://www.povray.org/). CCDC 731965 contains the supplementary crystallographic data for this paper. These data can be obtained free of charge from The Cambridge Crystallographic Data Centre via www.ccdc.cam.ac.uk/data_request/cif.

[10] I. D. Brown in *Structure and Bonding in Crystals*, *Vol. II* (Eds.: M. O'Keeffe, A. Navrotsky), Academic Press, New York, **1981**, pp. 1 – 30.

[11] a) The fact that an extensive butyrate uptake–release exchange in D_2O at room temperature (with reduced pore flexibility[12]) is not observable on the present time scale of NMR spectroscopy should be due to the presence of the rather large butyrates on both sides. In the latter context, the following observation should be mentioned: When ten equivalents acetic acid are added to a solution of 50 mg of the sodium salt of the butyrate capsule **1a** in D_2O at room temperature, or ten equivalents of *n*-butyric acid are added to the solution of the sodium salt of a capsule with acetate ligands (50 mg), uptake–release equilibria are observed in less than one hour. Note that in both cases the additional acid stimulates the exchange process (see Ref. [12b]). b) As the pK_a value of butyric acid at room temperature is 4.81 and the pH value of the investigated solution is about 4.0, most of the species called "free butyrates" in the text are protonated; for the pK_a, see *CRC Handbook of Chemistry and Physics: A Ready-Reference Book of Chemical and Physical Data*, 64th ed. (Ed.: R. C. Weast), CRC, Boca Raton, FL, **1984**. c) This is valid, for example, for bidentate ligands like acetates and oxalates coordinated to the {Mo_2} linkers but also for the ^{7}Li NMR spectroscopy signals of integrated Li^+ ions in the case of solutions of Li^+-type capsules.[8a–d]

[12] a) With the O···O separation of butyric acid of approximately 2.25 Å (F. J. Strieter, D. H. Templeton, *Acta Crystallogr.* **1962**, *15*, 1240 – 1244) and taking into account the van der Waals radii of the two oxygen atoms, we obtain a related value of the carboxylate group which is larger than the pore openings (ca. 3 Å; for details see Figure SI-5 in the Supporting Information). b) The qualitative observation of the related pore flexibility (see title) was mentioned earlier, for example, in Ref. [20] of T. Mitra, P. Miró, A.-R. Tomsa, A. Merca, H. Bögge, J. B. Ávalos, J. M. Poblet, C. Bo, A. Müller, *Chem. Eur. J.* **2009**, *15*, 1844 – 1852: "In this context it is important to note that this ligand exchange (acetate versus sulfate) is based on some flexibility of the pores regarding partial opening which is one of the most important properties of the capsules. […] At lower pH the acetate ligands get (upon addition of H_2SO_4) protonated while correspondingly leaving the capsule and sulfate ions are taken up" (for the corresponding synthesis, see A. Müller, Y. Zhou, H. Bögge, M. Schmidtmann, T. Mitra, E. T. K. Haupt, A. Berkle, *Angew. Chem.* **2006**, *118*, 474 – 479; *Angew. Chem. Int. Ed.* **2006**, *45*, 460 – 465). c) For more sophisticated evidence of pore widening, see the kinetic study in A. Ziv, A. Grego, S. Kopilevich, L. Zeiri, P. Miro, C. Bo, A. Müller, I. A. Weinstock, *J. Am. Chem. Soc.* **2009**, *131*, 6380 – 6382. But it has to be admitted that details about pore opening are not known.

[13] a) A. M. Todea, A. Merca, H. Bögge, J. van Slageren, M. Dressel, L. Engelhardt, M. Luban, T. Glaser, M. Henry, A. Müller, *Angew. Chem.* **2007**, *119*, 6218 – 6222; *Angew. Chem. Int. Ed.* **2007**, *46*, 6106 – 6110; b) A. Müller, *Nat. Chem.* **2009**, *1*, 13 – 14 (Feature article); c) C. Schäffer, A. Merca, H. Bögge, A. M. Todea, M. L. Kistler, T. Liu, R. Thouvenot, P. Gouzerh, A. Müller, *Angew. Chem.* **2009**, *121*, 155 – 159; *Angew. Chem. Int. Ed.* **2009**, *48*, 149 – 153.

[14] T. Douglas, M. Young, *Nature* **1998**, *393*, 152 – 155.

[15] a) A. J. Olson, Y. H. E. Hu, E. Keinan, *Proc. Natl. Acad. Sci. USA* **2007**, *104*, 20731 – 20736; b) J.-M. Lehn, *Supramolecular Chemistry: Concepts and Perspectives*, Wiley-VCH, Weinheim, **1995**; c) M. Fujita in *Comprehensive Supramolecular Chemistry*, *Vol. 9* (Eds.: J. L. Atwood, J. E. D. Davies, D. D. MacNicol, F. Vögtle), Pergamon, Oxford, **1996**, pp. 253 – 282 (note related subtitle: "Supramolecular Self-assembly through Coordination").

[16] See for example, a) M. Yoshizawa, J. K. Klosterman, M. Fujita, *Angew. Chem.* **2009**, *121*, 3470 – 3490; *Angew. Chem. Int. Ed.* **2009**, *48*, 3418 – 3438 and b) D. Ajami, J. Rebek, Jr., *Nat. Chem.* **2009**, *1*, 87 – 90). In the latter case it was stated in the graphical abstract: "Molecules confined to small volumes (e.g. "in self-assembled capsules") can contort themselves into unusual conformations that differ from those usually observed when no constraints are placed on them." Regarding the future of inorganic chemistry research under confined conditions, see also Ref. [13b].

[17] *NMR Spectroscopy Explained* (Ed.: N. E. Jacobsen), Wiley, Hoboken, **2007**.

[18] J. A. Ernst, R. T. Clubb, H.-X. Zhou, A. M. Gronenborn, G. M. Clore, *Science*, **1995**, *267*, 1813 – 1817.

